Journal of Power Sources, 6 (1981) 25 - 34

NON-LINEAR SIMULATION OF CURRENT DISTRIBUTION AND POTENTIAL PROFILE IN POROUS MANGANESE DIOXIDE ELECTRODES DURING DISCHARGE

NACHBILDUNG VON STROMVERTEILUNG UND POTENTIALPROFIL IN PORÖSEN BRAUNSTEIN-ELEKTRODEN WÄHREND DER ENTLADUNG

KARL-JOACHIM EULER, THE LATE ULRICH EULER and BURKHART SEIM

Arbeitsgruppe Technische Physik der Gesamthochschule Kassel, Heinrich-Plett-Str 40, D-3500 Kassel (F R G)

(Received November 7, 1979, in revised form March 31, 1980)

Summary

During the discharge of porous MnO_2 electrodes, the homogeneous electrode potential is disturbed. Potential profiles are formed which level out the initial current distribution. The formation of potential profiles is possible only within the range of existence of the MnO_x phase and the pH range of the electrolyte. The local potential deviations have been simulated by small dry cells, inserted in the electrical network imitating the porous electrode.

The potential profile growth in a non-linear electrical electrode analogue has been investigated. As a result, it can be stated that the shape of the potential profile develops fairly rapidly, during the first 20 h of a discharge lasting 100 h. Later on, its shape remains nearly unchanged, whereas its absolute level grows uniformly.

As soon as the results obtained here have been transformed into cylindrical electrode geometry, they will be compared with real cells of adequate size for chemical investigations of the current distribution. Some preliminary results show good agreement.

Überblick

Während der Entladung wird das homogene Potential in porösen Braunstein-Elektroden gestört. Potentialprofile bilden sich, welche die anfängliche Stromverteilung einebnen Die Entstehung von Potentialprofilen ist nur im Existenzbereich der MnO_x-Phase und im pH-Bereich des Elektrolyten möglich Die örtlichen Abweichungen des Potentials werden durch kleine Trockenbatterien nachgebildet, die in das elektrische Modell der porösen Elektrode eingesetzt werden.

Berichtet wird uber das Wachsen des Potentialprofils in einem nichtlinearen elektrischen Elektrodenmodell Als Resultat erhalt man, dass die Form des Potentialprofils sich ziemlich schnell ausbildet, z B in den ersten zwanzig Stunden einer hundertstundigen Entladung Spater bleibt die Form annahernd unverandert, wahrend die absolute Hohe gleichmassig wachst

Sobald die hier vorgelegten Resultate auf Zylindergeometrie abgebildet sind, werden wir sie mit nassanalytischen Messungen an hinreichend grossen Zellen vergleichen Einige vorlaufige Resultate zeigen gute Uebereinstimmung

---

1. Introduction

In a previous paper [1] the initial current distributions in various porous battery electrodes have been evaluated by the application of non-linear electric analogues. The most interesting result was the current distribution in a very thick (approx. 150 mm) dry battery electrode, consisting of an MnO_2 battery mix. The characteristics of the electrode are given in Table 1, together with the composition. A set of current distribution curves is given in ref. 1, Fig. 9, page 57.

These initial current distributions, however, are modified during discharge. Within a linear overvoltage approximation, this has already been verified for positive dry cell electrodes [2] and for several other battery electrodes [3]. In general, it can be stated that the initial non-uniform current distribution of MnO_2 electrodes is flattened out during cell discharge. This has been predicted [2] and later verified qualitatively [4].

The non-linear electrode analogue now developed [1] allows a deeper and better-founded insight into the discharge mechanism of porous dry cell positives. The very large thickness (L = 150 mm) for the simulation makes the characteristics of the system more apparent. It has to be mentioned that the magnitude of the potential profile grows approximately with the square of the thickness, L^2.

We restrict ourselves to semi-infinite, flat electrodes having lateral dimensions which are large compared with their thickness, L. The electrons and ions are fed from opposite borders. Electrons and ions migrate only along the thickness coordinate z Electronic, ρ_e, and ionic resistivity, ρ_i, of the electrode are kept time-independent, homogeneous and isotropic. The overvoltage $\eta(i)$ is approximated by a logarithmic law $\eta \sim \log i$, where i in mA/cm^3 is the volumetric discharge current density. The simulation of $\eta(i)$ is effected by semi-conducting pn diodes OA 20, as in ref. 1.

2. Potential forming

The manganese dioxide incorporated in dry batteries consists, in most cases, of poorly crystallized γ-MnO_2 having a fairly wide phase width. During

TABLE 1

Characteristics of the porous MnO_2 electrode investigated with the help of a non-linear analogue, partly after ref 1

Electrode		
black mix	70% of electrolytic MnO_2	
	10% of acetylene carbon black	
	10% of graphite powder	
	10% of NH_4Cl powder	
	wetted with binding electrolyte of	70% water
		20% NH_4Cl
		10% $ZnCl_2$
compressed in an automatic core pressing tool		
measured electronic resistivity	ρ_e = 2 0 ohm cm	
measured ionic resistivity	ρ_i = 7 5 ohm cm	
logarithmic overvoltage function, see ref 1		
thickness L = 150 mm	area element ΔA = 1 cm^2	
electric analogue, see Fig 1		
consisting of 15 equal parts 14 closed meshes, 1 bisected at both ends		
electronic resistors	R_e = 800 ohms each	
ionic resistors	R_i = 3000 ohms each	
overvoltage function simulated by pn diodes OA 20		
potential profile introduced by dry batteries IEC 4 F 15 special		
voltage surmount factor	r = 4 0*	
current degression factor	c = 0 010 cm^3	
resistor enlarging factor	$w = r/c$ = 400 cm^{-3}	
time reducing factor	$k = t_{real}\ t_{sim}$ = 1 12	

*The factors r and c serve to match the diode characteristics to the measured overvoltage function

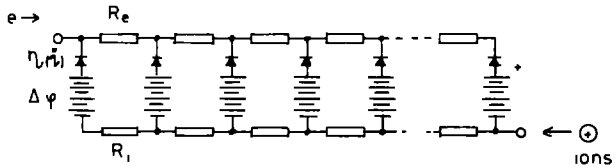

Fig 1 Electric analogue of a porous MnO_2 electrode, see Table 1 Electronic resistors R_e = 800 ohms each, electrons from the left, ionic resistors R_i = 3000 ohms each, ions from the right, overvoltage function, η_i, simulated by pn diodes in flux direction, potential profile, $\Delta\psi$, simulated by dry batteries IEC 4 F 15 special

cell discharge, the initial high degree, $x_o \approx 1.95$, of oxidation decreases continuously down to $x_f \approx 1.65$. This proceeds within the limits of one identical crystal modification, without forming a second phase. Thus, the chemical potential of the oxide decreases continuously also. In other words, the local single electrode potential, *e g.*, against zinc, is lowered depending on the electric charge taken out. As has been shown earlier [2], the potential may decrease more than 350 mV within the γ-MnO_x phase at constant pH.

The dry cell electrolyte consists of an aqueous solution of NH_4Cl and $ZnCl_2$ with small amounts of additives. Its initial pH $\approx$ 4.5 increases during cell discharge up to pH $\approx$ 9.5. This, again, causes a potential loss of approx. 280 mV. It depends in a rather complicated way on the discharge time, because several of the precipitated zinc compounds interact with the remaining solution, buffering the pH between 6 and 8, as has been shown by Cahoon [5]. The combination of the influence of the changes in the degree of oxidation and of the pH changes on the potential, results in the well-known decrease of the e.m.f. of dry cells, see Huber [6]. Also, the sum of both potential losses is the upper limit for the potential profile in monophase MnO_2 electrodes. In our case, the sum is 350 + 280 $\approx$ 630 mV. If in the undischarged centre of the porous electrode the degree of oxidation is still x_o = 1.95 at pH $\approx$ 4.5, and, at the same time, the edge is discharged to x_f = 1.65 at pH $\approx$ 9 5, the two local potentials differ by approx. 630 mV. In deeply discharged cells slightly larger potential differences may occur, because the influence of zinc ion concentration has not been considered so far, and because, possibly, the dehydration of the manganese dioxide influences the potential. Finally, the formation of a phase of very low degree of oxidation, Mn_3O_4 (hydro-hausmannite), cannot be excluded completely. In practical electrodes the potential profiles have a rather different magnitude, ranging from 50 mV in a fairly thin electrode [4] up to 800 mV observed here, see Fig. 4. The magnitude is approximately proportional to L^2, the square of the electrode thickness. The observation of potential profiles on electrochemical electrode models has been reported by Will [7].

3. Evaluation of local potential change

The local potential change, $\Delta\psi$, can hardly be measured because the necessary probes will disturb the potential field. We are able, however, to measure the potential change of thin electrodes of different thicknesses L_1 . L_2 ... . The results can be extrapolated to zero thickness, $L \to 0$. This procedure is not fully correct, because the influence of diffusion is neglected. To get a better approximation, we would have to insert the measured thin electrode between finite insulated layers of the same porosity. We tried to do this, but the procedure is quite complicated, and we were unable to get reproducible results. Thus, we prefer to use the extrapolated curves of single, thin electrodes, neglecting the diffusion. This approximation shows clearly the inherent limitation of the method used here.

Finely ground electrodeposited *manganese dioxide* of Japanese origin was dry mixed with 10% by weight of acetylene black, 10% of finely powdered graphite, and 10% of powdered NH_4Cl. The dry mix was wetted with an appropriate amount of electrolyte and carefully homogenized. After a rest period of 24 h, pellets of different thickness, L, between 1 and 10 mm were pressed. The tablets were furnished on one side with graphite tissue as the electrode terminal, and wrapped in bibulous paper. They were stored, if

necessary, under electrolyte, consisting of 70% by weight of water, 20% of NH_4Cl and 10% of $ZnCl_2$. The electrodes were discharged at 20 °C continuously at a constant current at about a 100 h rate in the same free, ungelled, electrolyte. The potential against Zn sheet has been recorded and extrapolated to zero thickness, $L \to 0$. The amount of electrolyte was fairly large in order to keep the rise of zinc concentration within limits. The Zn/Zn^{2+} potential, *e g*, against calomel reference electrodes, remained constant within the range of 20 mV. This small error was accepted, because Zn electrodes are much more convenient for practical purposes.

The curves are valid primarily for the special electrode formula and design given, but may also be regarded as an approximation for similar cases One difficulty seems to arise if the range of local current density exceeds the low current regime where the curve (a) of Fig. 2 has been taken. Under heavy load, the last part of the curves is changed considerably, but the first part of the discharge potential curves remains fairly unchanged.

The same black mix was used to measure electronic and ionic resistivity, ρ_e and ρ_i, respectively, as well as the overvoltage function $\eta(\iota)$, again extrapolated to zero thickness $L \to 0$. The techniques applied to get these data have been described several times in earlier publications, see, *e g*, refs. 2, 3. The results are given in Table 1, the overvoltage in the preceding publication [1].

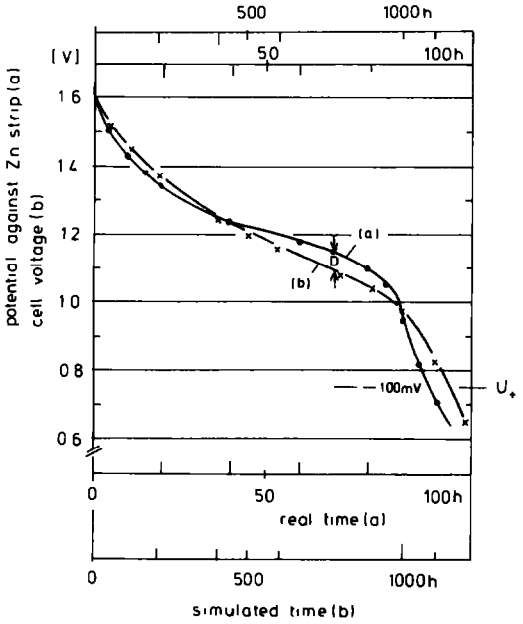

Fig 2 Representation of the potential drop during the discharge of the black mix, see Table 1 The simulated time is the real discharge time of the model (a) Desired curve, extrapolated to zero thickness, 100 h rate, (b) discharge curve of dry cell IEC F 15 special, 1200 h rate, D deviation, U_+ final voltage

4. Simulation of local potential changes

The potential drop evaluated has to be simulated and introduced into the electric analogue. In the case of manganese dioxide this is done by just using small dry batteries consisting of small, flat cells, International Electric Commission Standard IEC F 15. As shown in the preceding paper [1], a non-linear electric analogue has been used to investigate the current distribution in electrodes of uncommon thickness, see Table 1. The analogue had a voltage surmount factor $r = 4$. The voltage surmount, as defined in ref. 4, is the relation between the voltage drops in the model and in the real cell. Thus we used IEC 4 F 15 batteries consisting of four flat cells connected in series. As long as the discharge current remains below the range of the 100 h rate, its relative discharge curve remains fairly invariant against current changes, the voltage depending only on $Q = It$.

It must be mentioned that commercial IEC 4 F 15 batteries exhibit a fairly large internal resistance, ranging up to 1400 ohms at the end of a deep discharge, measured with low d.c. Therefore we used cells with a changed formula. In the black mix, 30% by weight of fine powder graphite was incorporated, and the usual electrolytic manganese dioxide was partly replaced by a very active, chemically prepared species. The electrolyte had a composition of 60% water, 25% NH_4Cl and 15% $ZnCl_2$. The zinc amalgamation was kept low, the separators as permeable as possible. These measures resulted in cells having a reduced shelf life of only a few weeks, and reduced capacity too, but a very low internal resistance, which could be neglected as being less than that of the overvoltage forming diode. To minimize self-discharge, the batteries have been cooled down to 8 °C in a household refrigerator. The battery was called IEC 4 F 15 special It had a diameter of 16 mm and a length of 35 mm, its weight was 11 g.

If the cell is discharged at the 1100 h rate, coinciding with the diode current in the electric analogue, its cell voltage only differs by less than $D \leqslant 10$ mV from the desired potential loss of the black mix during discharge, see Fig. 2, comparing curves (a) and (b).

Each sheet, Δz, of the electric analogue contains a pn diode. The local current density, *e g*, $\iota = 3$ mA/cm^3, to be simulated coincides with the diode current $I = 0.03$ mA Each sheet also contains a dry cell battery IEC 4 F 15 special which is discharged by the local diode current, *e g*, $I = 0.03$ mA in about $t_{sim} = 1150$ h = 48 days. The simulated current density $\iota = 3$ mA/cm^3 coincides, on the other hand, after a discharge time $t_{real} = 98$ h = 4 1 days, with the final voltage $U_+ = 0.75$ V, see Fig 2. The time scale therefore is enlarged by the factor $k = t_{real}\ t_{sim} = 1\ 12$. The discharge time of the model is about an order of magnitude *larger* than that of the real electrode t_{sim} is the actual discharge time of the model. The time lengthening depends little on the final voltage U_+, more on the choice of the active mass to be simulated, markedly on the properties of the battery incorporated in the model and considerably on the choice of the diode. To prevent self-discharge, the model has been discharged at 8 °C in a refrigerator.

As Fig. 2 shows, the wanted potential drop [1] does not fit exactly with the discharge voltage (b) of the batteries used. As long as the potential depends only on $Q = it_{real}$ and not on the load current density i, it seems possible to ameliorate it by the introduction of time-dependent reduction factors $k'(t_{real})$. Its variation in our case would be between 1 10 at t_{real} = 80 h and 1:12. However, we decided to use the constant k = 1:12 in the whole range, because we do not think that the misfit D causes an error of any importance in the general result.

5. Results and discussion

Figure 3 shows the current distribution for the porous MnO_2 electrode depending on the real discharging time t_{real}. The initial distribution is fairly steep and unsymmetrical. It fits, as expected, well to the distribution curves published in ref. 1. The centre of the electrode is discharged at less than 0 5 mA/cm^3 whereas the surface near the electrolyte is heavily loaded, more than 12 mA/cm^3. The relation of the current density between carbon and electrolyte borders is about $i_0 : i_L$ = 1:3. Near z = 10 cm a "shoulder" appears, which has also been observed in the previous paper [1]. It results from the introduction of the non-linear overvoltage functions. Certainly, the logarithmic approximation of the overvoltage coincides better with the electrochemical processes than the linear one does.

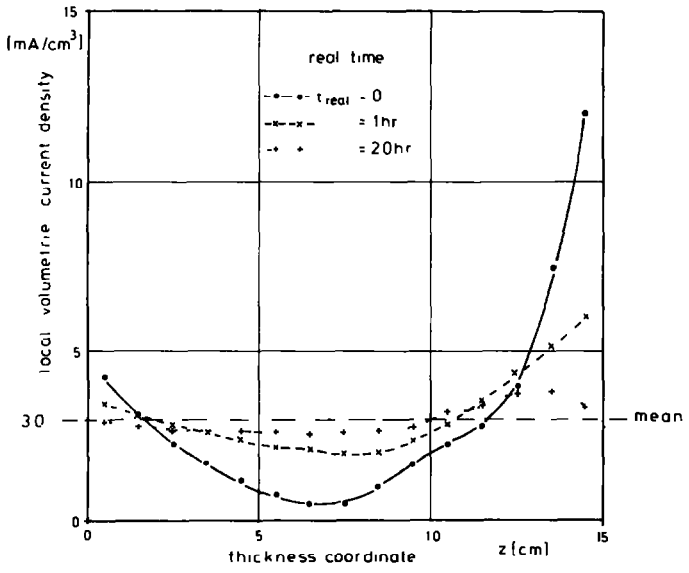

Fig 3 Current distribution in a porous MnO_2 electrode, see Table 1, depending on real time, t_{real} After 20 h of discharge, the distribution undergoes minor changes Electrons from the left, ions from the right side Discharge rate 100 h continuous, about 3 mA/cm^3

After 1 h of discharge, the current distribution is already much less pronounced. The current density at the centre of the electrode is now 2 mA/cm^3, and the unsymmetry relation is reduced to $i_o : i_L = 1:2$. After 20 h of discharge, the current distribution is fairly uniform, showing only a weak maximum at $z = 12.5$ cm and a very weak minimum in the centre. Continuing the discharge does not influence the current distribution further. It remains flat till the end of the discharge after 95 h. This behaviour is unexpected, because after 20 h the voltage between the terminals of the model is still 1.3 V, followed by a continuous decrease down to 0.75 V. Thus we expected, during the remaining discharge, a marked change in the current distribution.

As Fig. 4 shows, there is really a continuous growth of the potential profile. The initial profile is zero. After 1 h, a marked profile of about 100 mV has already been built up. After 20 h this has risen to about 250 mV Later on, its *shape* remains unchanged, only an additional potential drop appears, which does not depend on the thickness coordinate z. This explains the still unchanged current distribution after 20 h, because homogeneous potentials do not have any influence on the current distribution. On the other hand, the full profile magnitude influences the cell e.m.f.

We tried repeating the investigation of simulating porous MnO_2 electrodes with electric analogues using changed parameters, and we always

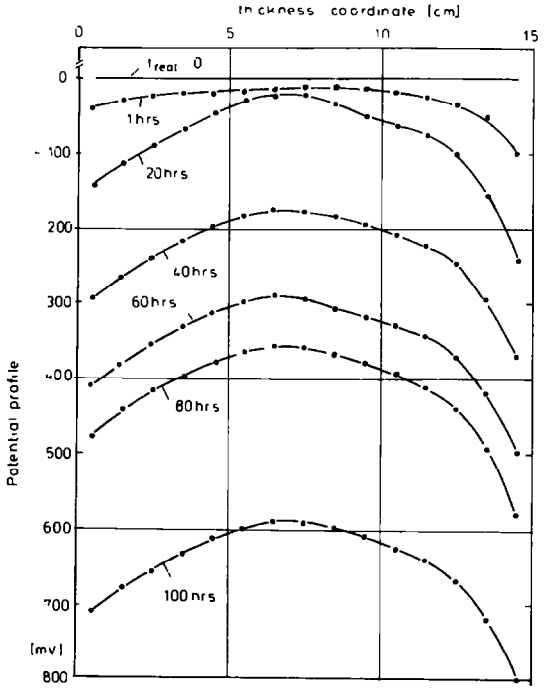

Fig 4 Potential profile in a porous MnO_2 electrode, see Table 1, depending on real time, t_{real} Discharge conditions as for Fig 3

obtained similar results. Thus, we assume that the results are significant and do not describe only the special case studied here. It is simply an example for porous MnO_2 electrodes in dry cells. The instrumental reproducibility is good, errors of only ±5% in current density and voltage have been observed. The critical question arises regarding the correct evaluation of the parameters, resistivities, overvoltage, e.m.f. decrease, etc. It is hardly possible to indicate their probable errors, but we hope that the parameters we used are characteristic for practical dry cell electrodes.

With this in mind, it can be stated that even in very thick, porous electrodes, potential profiles of only about 200 mV or less are sufficient to improve the current distribution markedly. This is in agreement with a publication of Formichev [8], who investigated the current distribution on the surface of non-equipotential bulk electrodes. The introduction of artificial potential profiles is possible, *e g.*, by the application of multilayer electrodes having different types of manganese dioxide in the different layers. The inner parts must be furnished with a high-potential manganese dioxide, whereas the outer parts contain low-potential material. The use of two-layer electrodes has already been reported. Possibly, however, a multilayer design may be of some practical advantage.

It must be added that the behaviour described above is characteristic only of MnO_2 electrodes. PbO_2, porous metal electrodes, HgO, etc., behave quite differently. These are characterized by narrow reaction zones migrating through the thickness of the electrode. This behaviour results in step-like potential profiles propagating from the face into the electrode

6. Comparison with real cells

The results of the simulation given above relate to very thick (L = 15 cm), flat electrodes having lateral dimensions which are large in comparison with the thickness. Thus, the experimental comparison of the results of the simulation with experimental cells would require very large electrode dimensions, *e g*, thickness L = 15 cm, area 60 × 60 cm^2. Therefore, we plan to apply a conformal mapping to the cylindrical geometry and to transform the planar thickness L into a radial thickness Δr of the outer and inner radii of a cylindrical electrode, having a carbon pencil in its centre. However, we are not sure that this rather rigorous mathematical treatment does not affect the results in an unacceptable manner, although we can state that some preliminary results we obtained using practical no. 6 cells are in close agreement with the predicted results of our simulation method. A straight-forward comparison will be published after the measurements and the chemical analysis have been completed.

Acknowledgements

The measurements were partly completed ten years ago at Frankfurt/M. in the research laboratory of the Varta Batterie AG. The authors thank Prof.

Dr. G. Lander for his kind permission to use these results. The remainder of the measurements and calculations have been done in the Working Group of Practical Physics of the University (Gesamthochschule) of Kassel. We are indebted to Mrs. Ursula Stassinet for preparing electrical analogues and to Dr Robert Kirchhof for measuring the powder properties.

References

1 K -J Euler and B Seim, Non-linear electric analogues of the current distribution in porous electrodes, *J Appl Electrochem , 8* (1978) 49 - 59
2 K -J Euler, Die Aenderung der Stromverteilung in poroesen Braunstein-Elektroden, *Electrochim Acta, 7* (1962) 205 - 223
3 K -J Euler, Die Aenderung der Stromverteilung in poroesen Elektroden, *Elektrochim Acta, 13* (1968) 1533 - 1549
4 K -J Euler, Zur Entwicklung des Potentials in einer poroesen Elektrode, *Z Angew Phys , 29* (1970) 264 - 265
5 N C Cahoon, Electrolyte equilibria in relation to dry cell performance, *Trans Electro chem Soc , 92* (1947) 159 - 172
6 R Huber, Leclanché Batteries, in K V Kordesch (ed), *Batteries,* Vol I, Marcel Dekker, New York, 1974, pp 1 - 239 See especially Figs 53 - 55 on pp 132 - 134
7 F G Will, Current distribution and pH gradients in a model of battery plate, in D H Collins (ed), *Power Sources 2,* Pergamon Press, Oxford, 1970, pp 149 - 165
8 V G Formichev, Current distribution at a non-equipotential electrode (in Russian), *Elektrokhimiya (Moscow), 4* (1968) 786 - 793